Supplementary Information for

Tunable synthesis of multiply-twinned intermetallic Pd_3Pb nanowire networks toward efficient N_2 to NH_3 conversion

Jingchun Guo,[a] Hui Wang,[b] Fei Xue,[c] Dan Yu,[b] Li Zhang,[b] Shilong Jiao,[a] Yihui Liu,[b] Yangfan Lu,[d] Maochang Liu,[c] Shuangchen Ruan,[a] Yu-Jia Zeng,*[a] Chao Ma,*[b] and Hongwen Huang*[bd]

[a] Shenzhen Key Laboratory of Laser Engineering, College of Physics and Optoelectronic Engineering, Shenzhen University, Shenzhen 518060, P.R. China.

[b] College of Materials Science and Engineering, Hunan University, Changsha, Hunan 410082, P. R. China.

[c] International Research Center for Renewable Energy, State Key Laboratory of Multiphase Flow in Power Engineering, Xi'an Jiaotong University, Xi'an, Shaanxi 710049, P.R. China.

[d] State Key Lab of Silicon Materials, School of Materials Science and Engineering, Zhejiang University, Hangzhou 310027, P. R. China.

Correspondence and requests for materials should be addressed to Y.-J.Z. (email: yjzeng@szu.edu.cn), C.M. (email: cma@hnu.edu.cn) or to H.H. (email: huanghw@hnu.edu.cn).

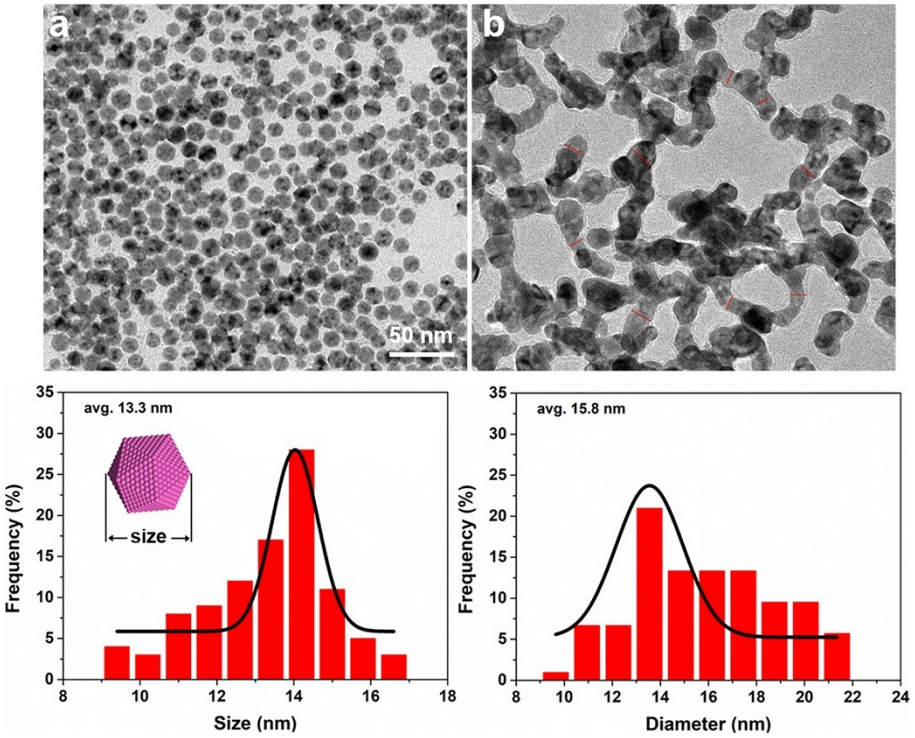

Supplementary Figure S1. The TEM images of Pd icosahedra with average sizes of (a) 13.3 nm and (b) the corresponding synthesized Pd_3Pb MT-IM-PNNs with average diameter of 15.8 nm. The scale bars in (a) and (b) are 50 nm as shown in (a). The red lines in (b) represent the diameter of MT-IM-PNNs.

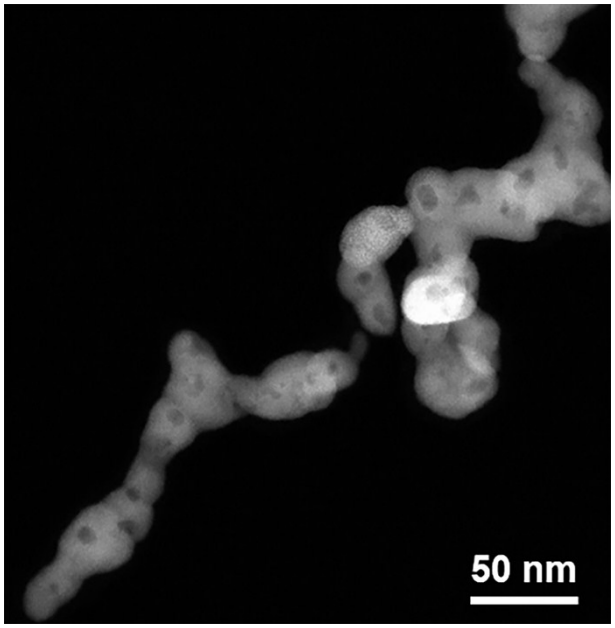

Supplementary Figure S2. Low-magnification HAADF-STEM image of Pd_3Pb MT-IM-PNNs.

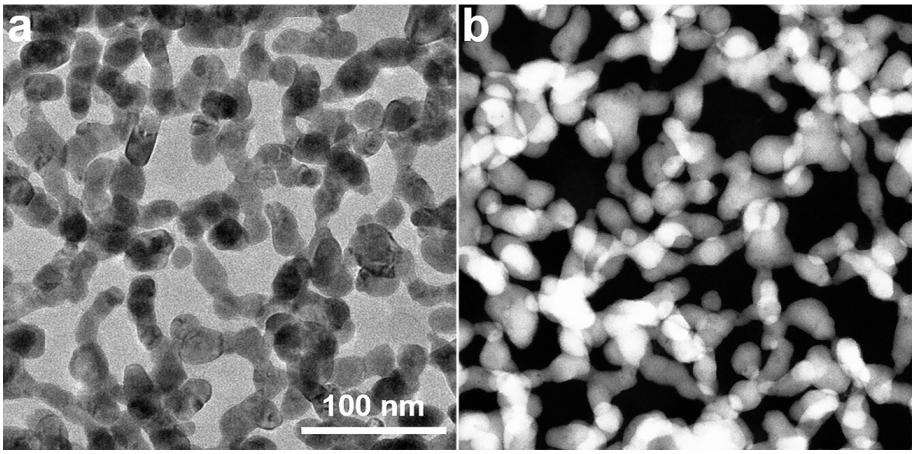

Supplementary Figure S3. (a) TEM image, and (b) Low-magnification HAADF-STEM image of Pd_3Pb MT-IM-NNs. The scale bars in (a) and (b) are 100 nm as shown in (a).

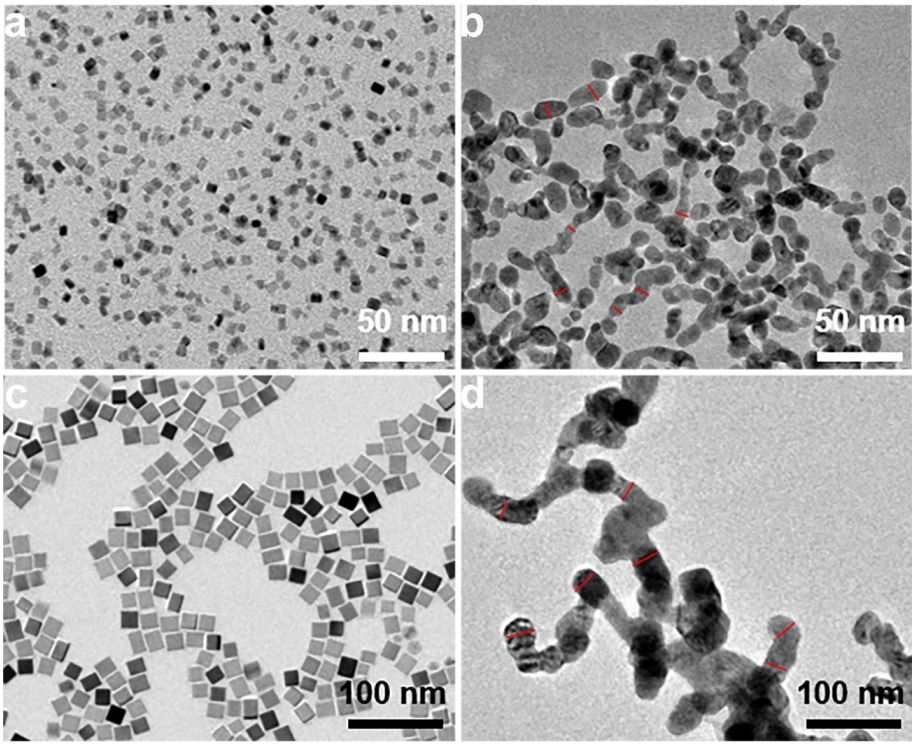

Supplementary Figure S4. The TEM images of Pd cubes with average sizes of (a) 5.7 nm and (c) 17.1 nm, respectively. (b) and (d) are the corresponding synthesized Pd_3Pb MT-IM-NNs.

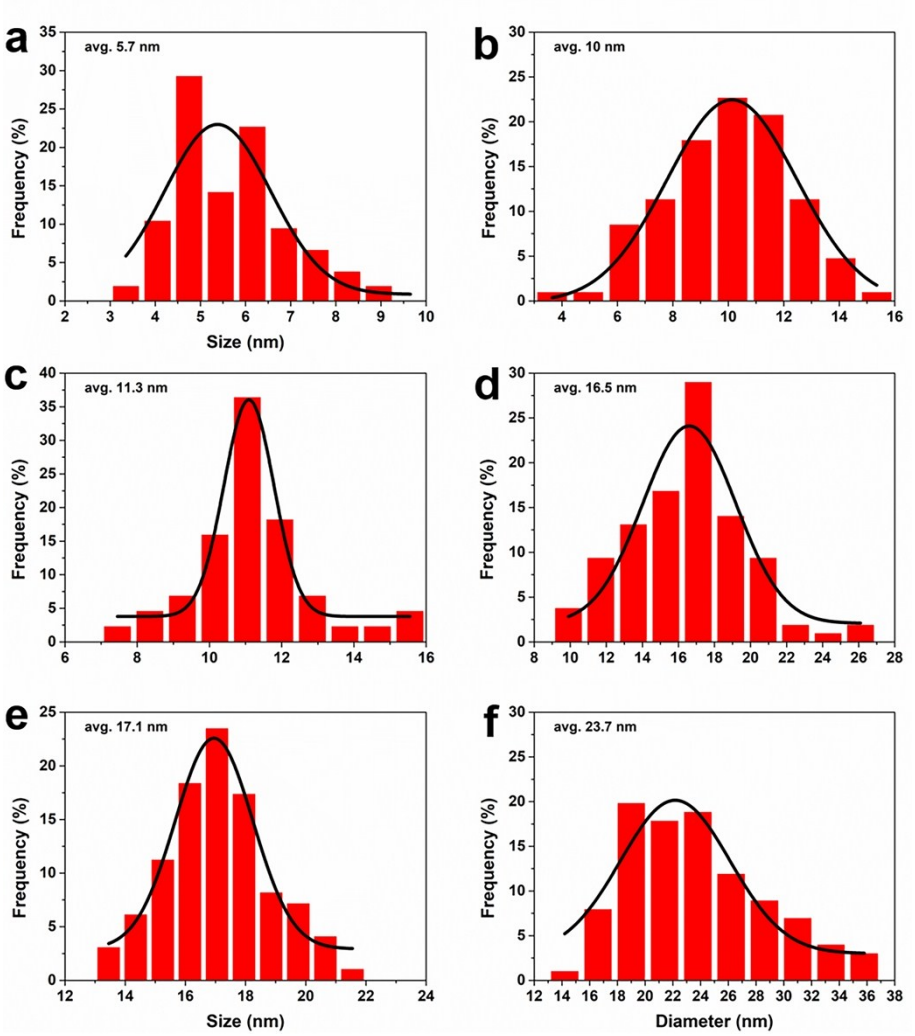

Supplementary Figure S5. The size distributions of different Pd cubes with average sizes of (a) 5.7 nm, (c) 11.3 nm and (e) 17.1 nm, respectively. (b), (d) and (f) are the diameter distributions of corresponding synthesized Pd_3Pb MT-IM-NNs with average diameters of (a) 10 nm, (c) 16.5 nm and (e) 23.7 nm, respectively.

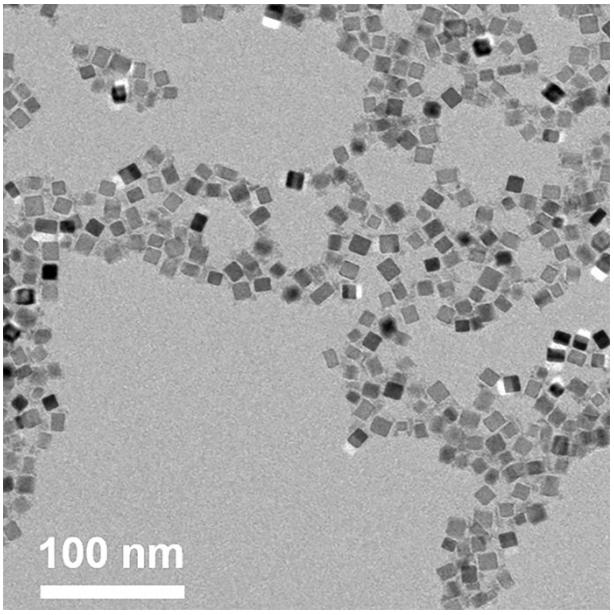

Supplementary Figure S6. The TEM images of Pd cubes, which were obtained by mixing 1.42 mg Pd cubes, 105 mg PVP and 4 mL DEG without $Pb(acac)_2$ at 180 ^oC for 24 h.

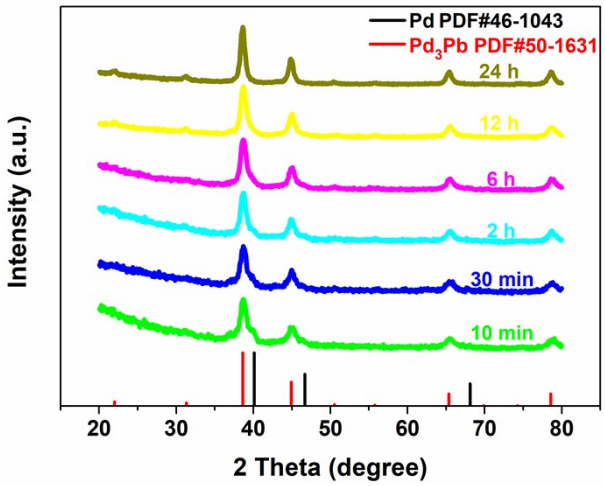

Supplementary Figure S7. Time-dependent XRD patterns of Pd_3Pb MT-IM-NNs.

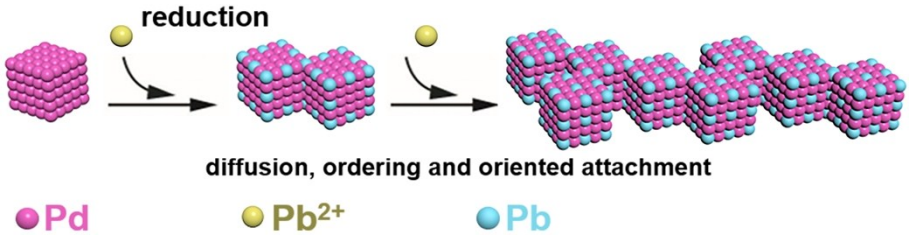

Supplementary Figure S8. Illustration of oriented-attachment formation mechanism using Pd cubes as seeds.

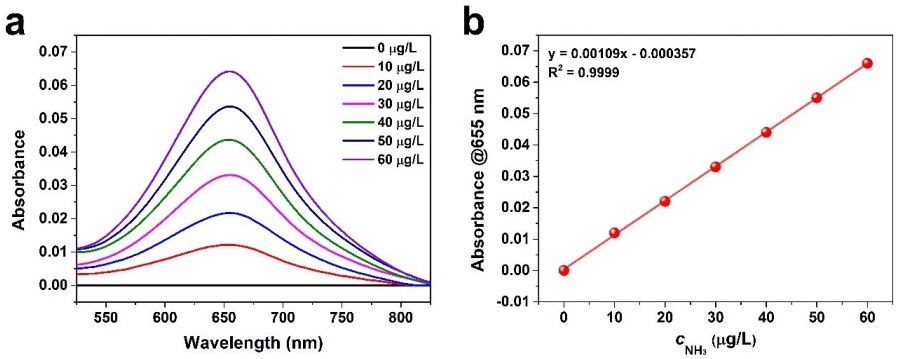

Supplementary Figure S9. Determination of the produced NH_3 in 0.1 M Na_2SO_4. (a) The UV-Vis absorption spectra of various concentrations of standard NH_4Cl solutions in the presence of 0.1 M Na_2SO_4 and (b) corresponding calibration curve for the colorimetric NH_3 assay using the indophenol blue method.

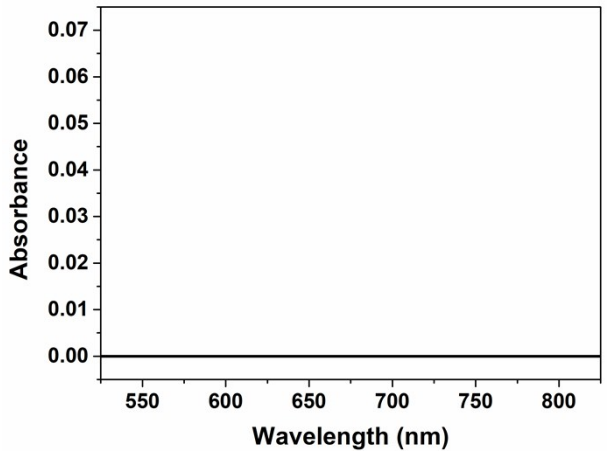

Supplementary Figure S10. The UV-Vis absorption spectrum of Na_2SO_4 electrolyte, which was performed by putting the working electrode of Pd_3Pb MT-IM-PNNs into N_2-saturated electrolyte for 2.5 hours with an open circuit.

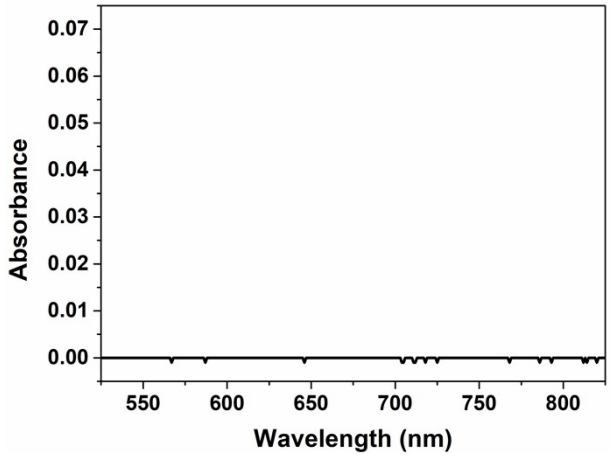

Supplementary Figure S11. The UV-Vis absorption spectrum of Na_2SO_4 electrolyte, which was performed by putting the working electrode of Pd_3Pb MT-IM-PNNs into Ar-saturated electrolyte with applied potential of -0.2 V vs RHE.

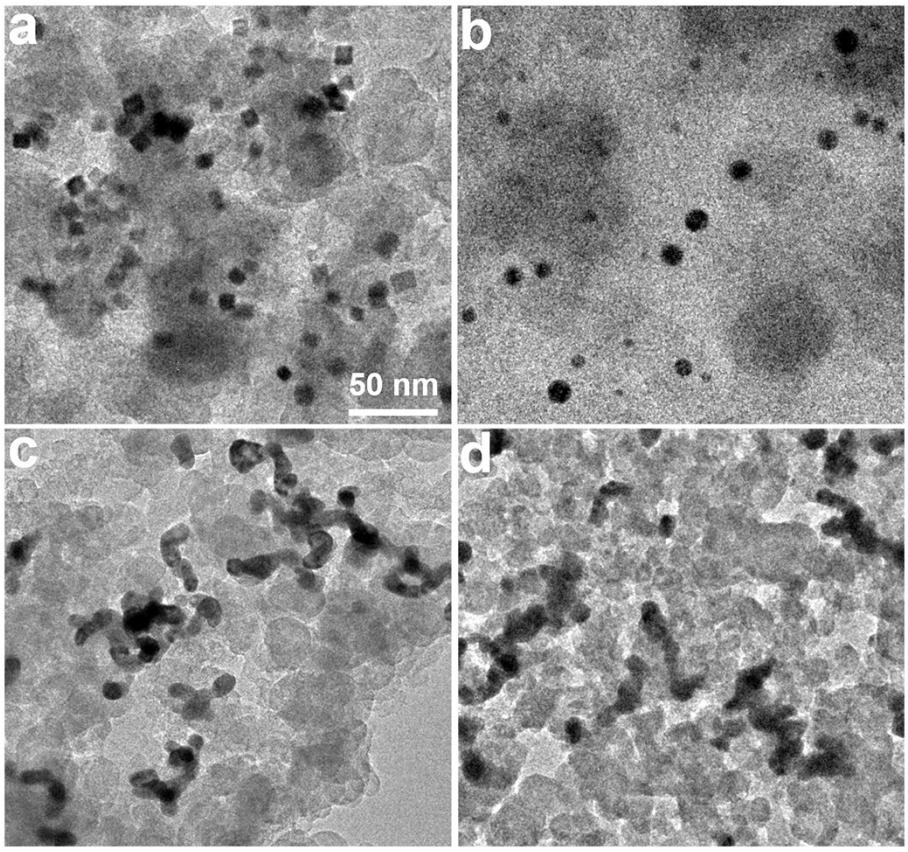

Supplementary Figure S12. TEM images of carbon black-supported (a) Pd cube, (b) Pd icosahedron, (c) Pd_3Pb MT-IM-NNs, and (d) Pd_3Pb MT-IM-PNNs, respectively. The scale bars are 50 nm as shown in (a).

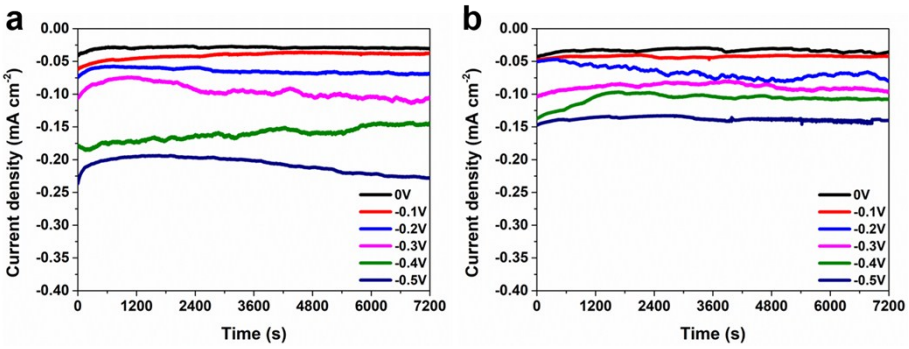

Supplementary Figure S13. Chronoamperometric curves of (a) Pd_3Pb MT-IM-PNNs and (b) Pd_3Pb MT-IM-NNs at the corresponding potentials in N_2-saturated 0.1 M Na_2SO_4 electrolyte.

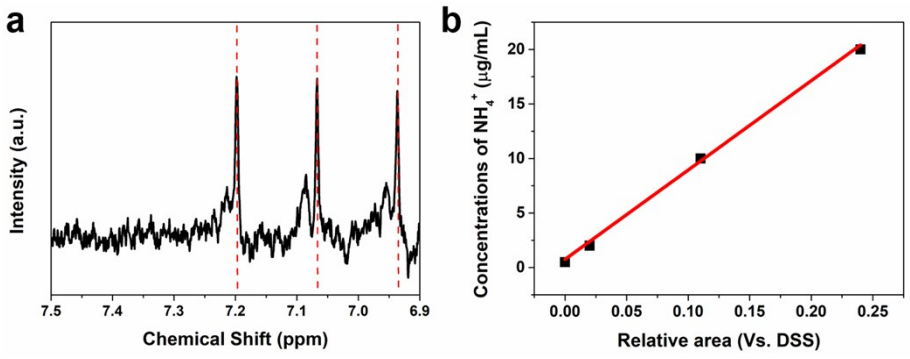

Supplementary Figure S14. (a) ^{1}H Nuclear magnetic resonance (NMR) spectrum of NH_4^+ in Na_2SO_4 electrolyte after 24 h of electrochemical NRR test with applied potential of -0.2 V vs RHE. The Na_2SO_4 electrolyte was concentrated from 30 mL to 0.5 mL to improve the signal-to-noise ratio. (b) Linear relationship between the NH_4^+ concentration and relative area vs. DSS. The standard curve was made as follows: A 0.5 mL of NH_4Cl solution with different concentration (from 0.5 to 20 μg/mL) was mixed with 0.1 mL D_2O and 0.1 mL 6 mM DSS solution added as an internal standard.

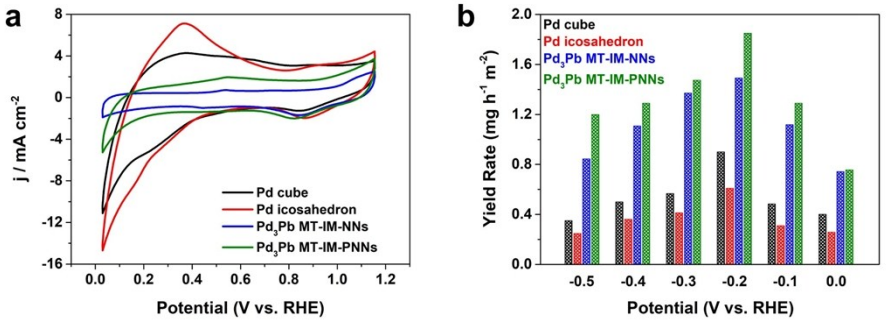

Supplementary Figure S15. (a) CV curves of Pd cube (black), Pd icosahedron (red), Pd_3Pb MT-IM-NNs (blue), and Pd_3Pb MT-IM-PNNs (olive) electrodes in N_2-saturated 0.1 M KOH electrolyte at a scan rate of 50 mV/s. (b) The NH_3 yield rates normalized by calculated ECSAs of Pd cube (black), Pd icosahedron (red), Pd_3Pb MT-IM-NNs (blue), and Pd_3Pb MT-IM-PNNs (olive).

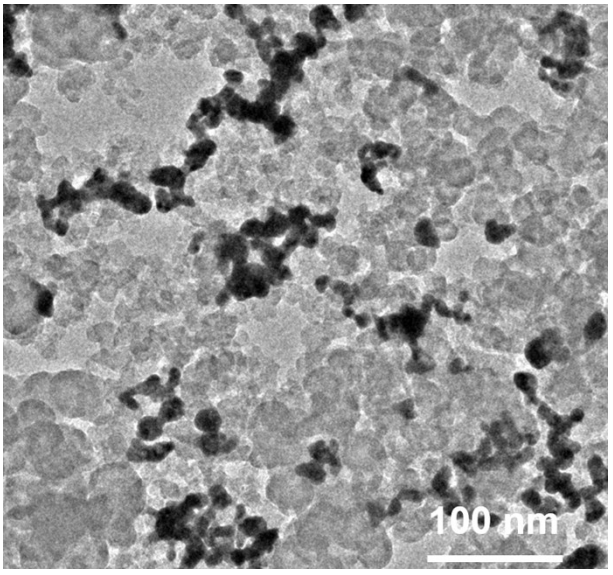

Supplementary Figure S16. TEM images of carbon black-supported Pd_3Pb MT-IM-PNNs after stability test.

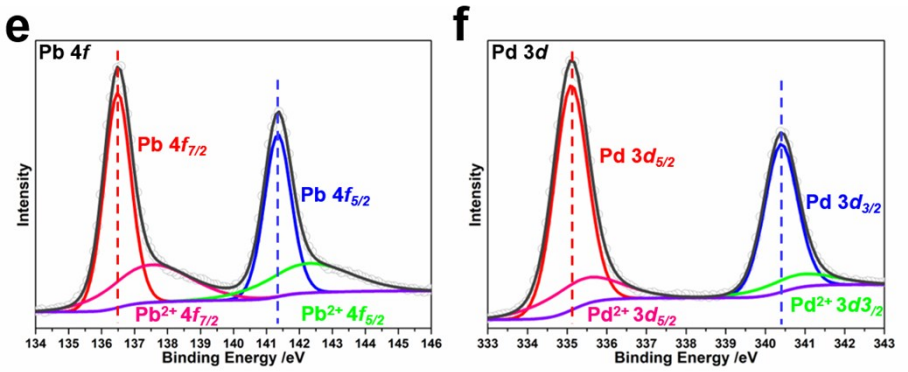

Supplementary Figure S17. XPS of (e) Pb 4f and (f) Pd 3d spectra of Pd_3Pb MT-IM-PNNs after NRR test.

Supplementary Table S1. Comparison of the NRR performance of Pd_3Pb MT-IM-PNNs with other electrocatalysts under ambient conditions.

Catalyst	Electrolyte	Potential (V vs. RHE)	Faradaic efficiency (%)	Yield rate ($\mu g\ h^{-1}\ mg_{cat}^{-1}$)	Ref.
Noble metal-based electrocatalyst					
Pd_3Pb MT-IM-HNWs	0.1 M Na_2SO_4	-0.2	21.46	18.2	This work
Au nanorods	0.1 M KOH	-0.2	3.88	1.648	1
Au Sub-Nanoclusters	0.1 M HCl	0.2	8.11	21.4	2
Au Nanoparticles	0.1 M PBS	0.1	8.2	4.4	3
Rh nanosheet	0.1 M KOH	-0.2	0.217	23.88	4
$Pd_{0.2}Cu_{0.8}$ Nanocluster	0.1 M KOH	-0.2	0.7	2.8	5
Pd nanoparticles	0.1 M PBS	0.1	8.2	4.5	6
Pd_3Cu_1 alloy	0.1 M KOH	-0.25	1.22	39.9	7
Noble metal-free electrocatalyst					
$Bi_4V_2O_{11}/CeO_2$	0.1 M HCl	-0.2	10.16	23.21	8
MoS_2 nanoflower	0.1 M Na_2SO_4	-0.4	8.34	29.28	9
Mo_2C/C nanosheets	0.5 M Li_2SO_4	-0.3	7.8	11.3	10
Nb_2O_5 nanofiber	0.1 M HCl	-0.55	9.26	43.6	11
Hollow Cr_2O_3 microspheres	0.1 M Na_2SO_4	-0.9	6.78	25.3	12
$BiVO_4$	0.2 M Na_2SO_4	-0.5	10.04	8.6	13
Metal-free electrocatalyst					
B_4C nanosheet	0.1 M HCl	-0.75	15.59	26.57	14
Carbon nitride	0.1 M HCl	-0.2	11.59	8.09	15
N-doped porous carbon	0.1 M HCl	-0.2	1.45	15.7	16
Mesoporous boron nitride	0.1 M Na_2SO_4	-0.7	5.5	18.2	17

Supplementary References

(1) D. Bao, Q. Zhang, F. Meng, H. Zhong, M. Shi, Y. Zhang, J. Yan, Q. Jiang, and X. Zhang, *Adv. Mater.* 2017, **29**, 1604799.

(2) M. Shi, D. Bao, B. Wulan, Y. Li, Y. Zhang, J. Yan, and Q. Jiang, *Adv. Mater.* 2017, **29**, 1606550.

(3) S. Li, D. Bao, M. Shi, B. Wulan, J. Yan, and Q. Jiang, *Adv. Mater.* 2017, **29**, 1700001.

(4) H. Liu, S. Han, Y. Zhao, Y. Zhu, X. Tian, J. Zeng, J. Jiang, B. Xia, and Y. Chen, *J. Mater. Chem. A*. 2018, **6**, 3211–3217.

(5) M. Shi, D. Bao, S. Li, B. Wulan, J. Yan, and Q. Jiang, *Adv. Energy Mater.* 2018, **8**, 1800124.

(6) J. Wang, L. Yu, L. Hu, Xin, G. Chen, H. Xin, and X. Feng, *Nat. Comm*. 2018, **9**, 1795.

(7) F. Pang, Z. Wang, K. Zhang, J. He, W. Zhang, C. Guo, and Y. Ding, *Nano Energy* 2019, **58**, 834–841.

(8) C. Lv, C. Yan, G. Chen, Y. Ding, J. Sun, Y. Zhou, and G. Yu, *Angew. Chem. Int. Ed*. 2018, **57**, 6073–6076.

(9) X. Li, T. Li, Y. Ma, Q. Wei, W. Qiu, H. Guo, X. Shi, P. Zhang, A. Asiri, L. Chen, B. Tang, and X. Sun, *Adv. Energy Mater*. 2018, **8**, 1801357.

(10) H. Cheng, L. Ding, G. Chen, L. Zhang, J. Xue, and H. Wang, *Adv. Mater.* 2018, **30**, 1803694.

(11) J. Han, Z. Liu, Y. Ma, G. Cui, F. Xie, F. Wang, Y. Wu, S. Gao, Y. Xu, and X. Sun, *Nano Energy* 2018, **52**, 264–270.

(12) Y. Zhang, W. Qiu, Y. Ma, Y. Luo, Z. Tian, G. Cui, F. Xie, L. Chen, T. Li, and X. Sun, *ACS Catal.*, 2018, **8**, 8540–8544.

(13) J. Yao, D. Bao, Q. Zhang, M. Shi, Y. Wang, R. Gao, J. Yan, and Q. Jiang, *Small Methods* 2018, 1800333.

(14) W. Qiu, X. Xie, J. Qiu, W. Fang, R. Liang, X. Ren, X. Ji, G. Cui, A. Asiri, G. Cui, B. Tang, and X. Sun, *Nat. Commun.*, 2018, **9**, 3485.

(15) C. Lv, Y. Qian, C. Yan, Y. Ding, Y. Liu, G. Chen, and G. Yu, *Angew. Chem., Int. Ed.*, 2018, **57**, 10246–10250.

(16) X. Yang, K. Li, D. Cheng, W. Pang, J. Lv, X. Chen, H. Zang, X. Wu, H. Tan, Y. Wang, and Y. Li, *J. Mater. Chem. A*, 2018, **6**, 7762–7769.

(17) J. Zhao, X. Ren, X. Li, D. Fan, X. Sun, H. Ma, Q. Wei, and D. Wu, *Nanoscale*, 2019, **11**, 4231–4235.